

## انزلاق خرزة علي منحني أملس لقطع مكافئ رأسي يدور بسرعة زاوية منتظمة: توصيف الاستقرار

جلال محروس معتمد

قسم الرياضيات، كلية التربية، جامعة عين شمس، القاهرة، مصر

### الملخص

هذا البحث يدرس حركة الخرزة الانزلاقية على سطح أملس، تم تدوير المنحني حول محوره العمودي بتردد زاوي منتظم. المعادلة التي تتحكم بالحركة غير خطية بشكل كبير. تم استخدام طريقة الاضطراب الهموتوبي وتحويلات لابلاس . إيجاد الحل التقريبي لحركة خرزة علي منحني أملس علي شكل قطع مكافئ محوره رأسي حيث يدور حول محوره بسرعة زاوية منتظمة وذلك باستخدام طريقة الاضطراب الهموتوبي وتحويلات لابلاس. باستخدام مفهوم تمديد التردد الطبيعي، تم الحصول علي الحل التقريبي الدوري، وكذلك الحصول علي معيار الاستقرار. وباعتبار عجلة الجاذبية الأرضية دالة دورية مع الزمن، تم إثارة المنظومة والحصول علي الحل التقريبي مرة أخرى باستخدام طريقة القياس الزمني المتضاعف. تم أيضاً استخدام طريقة التحليل الخطي للاستقرار لمقارنة النتائج في الحالتين الاخيرتين. من الحسابات العددية، تمكنا من تحديد أدوار البرامترات الفيزيائية الحاكمة للحركة في إحداث استقرار الاتزان من عدمه.

# Sliding bead on a smooth vertical rotated parabola: stability configuration

Galal M. Moatimid

*Dept. of Mathematics, Faculty of Education, Ain Shams University, Roxy, Cairo*

*Corresponding author: gal\_moa@hotmail.com*

## Abstract

This paper investigates the motion of a sliding bead on a smooth vertical parabola. The parabola is rotated about its vertical axis with a uniform angular frequency. The governing equation of motion is a highly nonlinear second-order ordinary differential equation. An approximate solution is achieved via the coupling of the homotopy perturbation method and Laplace transform. On the other hand, an expanded frequency concept is utilized in order to obtain an approximate periodic solution. Therefore, the expanded frequency method is applied to govern the stability criterion of the problem. An external excitation of the problem is examined through an additional oscillatory gravitational force. The multiple time-scales with the homotopy perturbation method are used to judge the stability criteria. The analyses reveal the resonance together with the non-resonant cases. Furthermore, the linearization techniques are utilized to check the stability of the linearized equation and to compare the findings with those obtained in the multiple time-scales. Numerical calculations are performed to graphically illustrate, the perturbed solutions as well as the stability examination. It is found that the initial and angular velocities have a destabilizing influence. In contrast, the parameter of the reciprocal of the latus rectum has a stabilizing effect.

**Keywords:** Expanded frequency analysis; homotopy perturbation methods; Laplace transforms; multiple time-scales technique.

## 1. Introduction

The topic of the differential equations is a well-constructed part of mathematics. Many recent advances in mathematics have indicated that many phenomena in applied science are usually modeled by differential equations. The solutions of these equations yield some mathematical explanation. In other words, differential equations are arising naturally to form the foundations of science and engineering. They are considered as useful tools for solving physical problems. Nonlinear oscillator models have been widely used in several areas. They are significant in physics and engineering. Mechanical oscillatory systems are sometimes governed by nonlinear differential equations. Many problems in mathematical physics, chemical physics, and astrophysics are modeled by second-order nonlinear differential equation. Very few exact solutions for differential equations may be obtained in many branches of fluid mechanics, solid mechanics, physics, and engineering in accordance with the existence of nonlinearity, inhomogeneity, and variable coefficients. It is well-known that the existence and uniqueness of solutions of the nonlinear differential equations may be

studied by means of general theorems (see, for instance, Coddington & Levinson, 1977). On the other hand, there are many nonlinear ordinary differential equations that have no exact solutions in compact forms. Therefore, many authors have focused on obtaining analytical approximate/numerical solutions.

This paper focuses on the analytical approximate solution. Nayfeh and Mook (1979) discussed this topic. The well-known analytical approaches applied to solve nonlinear problems, in various situations, are called the perturbation methods (Nayfeh, 1973). These methods are based on the existence of a small parameter. Consequently, by means of this small parameter, the approximate solution may be expanded into an infinite number of linear sub-problems. This small parameter governs the accuracy of the perturbed approximation and achieves the validity of the perturbation method (Nayfeh, 1973). Through an analytical perturbation method, the small parameter should be exerted in the equation. Therefore, finding a small parameter in the differential equation is rather difficult. To overcome this shortcoming, many techniques have been postulated. Demiray and Bulut (2017) obtained exact

solutions involving the Jacobi elliptic function, hyperbolic function and a periodic wave solution for the generalized Gardner equation. This equation can be applicable in electromagnetic theory, special relativity, and heat transfer in several fields of physics.

As stated above, the perturbation method needs a small parameter to be utilized. However, the homotopy perturbation method (HPM) does not need the existence of any small parameter. It introduces an artificial imbedding parameter  $\rho \in [0,1]$ . The method provides an analytical approximate solution of different types of linear and nonlinear equations. The results indicate that the method is very effective, powerful and simple in obtaining approximate solutions of nonlinear differential equations. The HPM was first proposed by He (1999; 2000) for solving differential, integral and integro-differential equations. It has been the subject of extensive analysis and numerical works. In fact, the method is a coupling of the traditional perturbation method and homotopy in topology (He, 2000). The method has a significant advantage in that it provides analytical solutions to a wide range of nonlinear problems in engineering and physics.

In recent years, the application of the HPM in nonlinear problems had been studied by scientists and engineers because of its simplification in handling these problems. Because HPM becomes a powerful mathematical tool, researchers are using it to solve a wide variety of problems. Bayat *et al.*, (2015) used the HPM to obtain analytical solutions for three different examples. In addition, they compared their solutions with the energy balance method and the Runge-Kutta algorithm. They concluded that the HPM does not need any linearization and overcomes the limitations of the regular perturbation methods. Recently, El-Dib and Moatimid (2018) adapted the HPM to obtain exact solutions of linear and nonlinear differential equations. The basic idea to the approach is to choose a suitable trial function, usually in the form of a power series. The vanishing of the first order approximate solution guarantees that all higher orders are also canceled. Accordingly, the remaining zero-order solution is supported to become an exact one.

The method of Laplace transforms ( $L_T$ ) has been considered as a valuable tool in dealing with problems related to the linear systems involving integro-differential equations with constant coefficients, ordinary, partial and difference equations. Laplace first proposed this approach around 1820. His technique has played an important role

in mathematics for its theoretical interest and because it is a simpler fashion for solving problems in the sciences and engineering when compared to other mathematical techniques (Schiff, 1999). Ali *et al.*, (2017) derived exact solutions by using the  $L_T$  in terms of the Wright function. Furthermore, they illustrated the solutions throughout a set of diagrams of different physical parameters. Filobello-Nino *et al.*, (2017) proposed an application of the  $L_T$  with HPM when obtaining an analytical approximate solution for nonlinear differential equations with variable coefficients.

Parametric excitation in a mechanical system happens if a parameter of the system becomes time-dependent. The mathematical modeling of this type of excitation is characterized by means of differential equations which have time-dependent coefficients. A standard example of an equation which displays parametric excitation is the Mathieu equation. Parametric instability occurs when an external excitation appears as a coefficient of the system parameters. Under the periodic excitation instability, the excitation frequency approaches twice the natural frequency of the system. Ibrahim (1985) and Dao *et al.*, (2007) studied a Van der Pol oscillator under parametric and forced excitations. Their studies include a small parameter. It is a quasi-linear general case (without the assumption of the smallness of nonlinear terms and perturbations). Maiybaev (2002) studied a linear multi-parameter non-conservative system under small periodic parametric excitation. He derived approximations of the stability domain in a parameter space when the corresponding autonomous system has a zero eigenvalue or a pair of complex conjugate imaginary eigenvalues. Furthermore, the singularities that arise on the boundary of stability were analyzed. Kaliji *et al.*, (2013) presented two new analytical techniques named the max–min approach and iteration perturbation method for solving nonlinear equations of two oscillatory systems. One case consisted of a mass grounded by linear and nonlinear springs in a series, and the other one was a rigid rod that rocks on a circular surface. They obtained highly accurate analytical solutions for the free nonlinear vibration of conservative oscillations. They also investigated the dynamic behavior of the systems.

It should be noted that, in example 7.7 on page 245 of the book “Classical Dynamics of Particles and Systems”, (Thornton and Marion 2004) introduced the equation of the motion of a sliding bead over a smooth

vertical parabola. The parabola was assumed to rotate around its vertical axis by a uniform angular velocity. This investigation focuses on the stability profile of this problem. The goal was to obtain approximate solutions in different approaches. In addition, a stability profile was achieved. The paper begins with the methodology of the problem, and a simple derivation of the equation of motion is presented in Section 2. Section 3 shows how an approximate solution of the highly nonlinear equation via a coupling of the HPM and  $L_T$  was obtained. The periodic solution, based on the nonlinear frequency analysis, is reported in Section 4. An external parametric excitation under a vertical oscillating gravity is introduced in Section 5. Furthermore, the stability analysis, based on the multiple-time scales with HPM, is presented. The analysis covers the resonance and non-resonant cases. The linearization technique used to check the stability of the linearized equations is the focus of Section 6. Section 7 is devoted to the numerical calculations of all outcomes. This Section illustrates the approximate solutions as well as stability profiles. Concluding remarks can be found in Section 8.

## 2. Methodology

This paper focuses on (example 7.7 page 245) in the book of (Thornton and Marion 2004). For clarification, the problem under consideration consists of a bead which slides on a smooth wire which is bent in the shape of a vertical parabola in the form of  $z = cr^2$  (Fig. 1). The parabola is assumed to rotate about its vertical axis with a uniform angular velocity  $\omega$ . For more convenience, the cylindrical polar axes  $(r, \theta, z)$  are taken into account so that the vertical axis lies along the  $z$ -axis. The motion of the bead is acted upon by the gravitational acceleration which acts on the negative  $z$ -axis.

The Lagrangian function may be constructed as dependent only on the generalized coordinate  $r$  as follows:

$$L = \frac{m}{2} (\dot{r}^2 + 4c^2 r^2 \dot{r}^2 + r^2 \omega^2) - mgr^2. \quad (1)$$

Therefore, the Euler-Lagrange's equation of motion becomes

$$\ddot{r} (1 + 4c^2 r^2) + 4c^2 r \dot{r}^2 + r(2gc - \omega^2) = 0, \quad (2)$$

which is a highly nonlinear second-order differential equation.

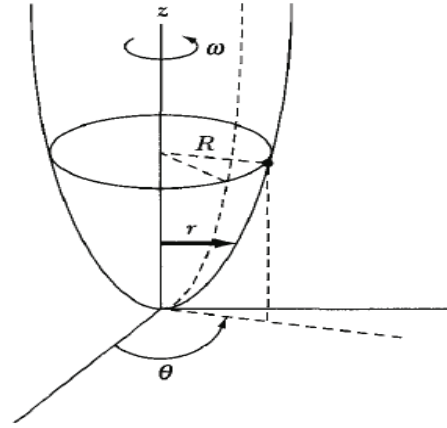


Fig. 1. Description of the problem.

A similar equation was analyzed by Wu *et al.*, (2003). The authors combined the linearization of the governing equation with the method of harmonic balance to establish an approximate analytical solution. They showed that the obtained approximate solutions were valid for small and large amplitudes of oscillation.

To achieve the approximate solution, it is convenient to assume the following initial conditions:

$$r(0) = 0, \text{ and } \dot{r}(0) = u. \quad (3)$$

As a special case, if the particle rotates on a circle  $r = R$ , then  $\dot{r} = \ddot{r} = 0$ , it follows that the equation of motion in (2) becomes

$$R(2gc - \omega^2) = 0 \text{ or } \omega = \sqrt{2gc}. \quad (4)$$

## 3. An approximate solution via the coupling of HPM and $L_T$

It should be noted that it is difficult to find the solution of some nonlinear differential equations in a compact form. For this reason, analytic approximations can be used to find their solutions. Therefore, because of the high nonlinearity of the equation of motion that is given in Equation (2), and as shown in the introduction, there are many perturbation methods to treat similar equations. In the following analysis, the treatment of this equation will be based on coupling the HPM and  $L_T$  as follows:

The linear and nonlinear parts of Equation (2) may be chosen as:

$$L(r) = \ddot{r} + \sigma^2 r \text{ and } N(r) = 4c^2 (r^2 \ddot{r} + \dot{r}^2) - \omega^2 r, \quad (5)$$

where  $\sigma^2 = 2gc$ .

It follows that the homotopy equation may be formulated as follows:

$$\ddot{r} + \sigma^2 r + 4c^2 \rho \left( r^2 \dot{r} + r \dot{r}^2 - \frac{\omega^2}{4c^2} r \right) = 0; \rho \in [0, 1], \quad (6)$$

where  $\rho$  is the embedding homotopy parameter.

Therefore, the function  $r(t)$  may be written as  $r(t) = r(t; \rho)$ . Applying the  $L_T$  on the homotopy Equation (10), one gets

$$(s^2 + \sigma^2) L_T \{r(t; \rho)\} - sr(0) - \dot{r}(0) = -\rho L_T \{N(r(t; \rho))\}. \quad (7)$$

On using the initial conditions that are given in Equation (3), one finds

$$L_T \{r(t; \rho)\} = \frac{u}{s^2 + \sigma^2} - \frac{\rho}{s^2 + \sigma^2} L_T \{N(r(t; \rho))\}. \quad (8)$$

The inverse Laplace transform of Equation (8), resulted in

$$r(t; \rho) = \frac{u}{\sigma} \sin(\sigma t) - \rho L_T^{-1} \left\{ \frac{1}{s^2 + \sigma^2} L_T \{N(r(t; \rho))\} \right\}. \quad (9)$$

In accordance with the regular HPM, the dependent function  $r(t; \rho)$  may be expanded as:

$$r(t; \rho) = \sum_{n=0}^{\infty} \rho^n r_n(t). \quad (10)$$

Accordingly, the nonlinear part  $N(r)$  should be written as follows:

$$N \left( \sum_{n=0}^{\infty} \rho^n r_n \right) = N_0(r_0) + \rho N_1(r_0, r_1) + \rho^2 N_2(r_0, r_1, r_2) + \dots + \rho^k N_k(r_0, r_1, r_2, \dots, r_k), \quad (11)$$

where

$$N_k(r_0, r_1, r_2, \dots, r_k) = \frac{1}{k!} \lim_{\rho \rightarrow 0} \frac{\partial^k}{\partial \rho^k} N \left( \sum_{n=0}^{\infty} \rho^n r_n(t) \right). \quad (12)$$

Inserting equations (10) and (11) into Equation (9), then equating the coefficients of like powers of  $\rho$  on both sides, one gets the following equations:

$$\rho^0: r_0(t) = \frac{u}{\sigma} \sin(\sigma t), \quad (13)$$

$$\rho: r_1(t) = -L_T^{-1} \left\{ \frac{1}{s^2 + \sigma^2} \left\{ L_T \left[ 4c^2 (r_0^2 \ddot{r}_0 + r_0 \dot{r}_0^2) - \omega^2 r_0 \right] \right\} \right\}, \quad (14)$$

and

$$\rho^2: r_2(t) = -L_T^{-1} \left\{ \frac{L_T}{s^2 + \sigma^2} \left\{ 4c^2 (r_0^2 \ddot{r}_1 + 2r_0 r_1 \ddot{r}_0 + 2r_0 \dot{r}_0 \dot{r}_1) \right\} \right\} \quad (15)$$

Clearly, the solution of each order depends mainly on the previous one.

Using the Mathematica, the following results can be obtained:

$$r_1(t) = \frac{u(c^2 u^2 + 2\omega^2)}{4\sigma^3} \sin(\sigma t) - \frac{ut(2c^2 u^2 + \omega^2)}{2\sigma^2} \cos(\sigma t) + \frac{c^2 u^3}{4\sigma^3} \sin(3\sigma t), \quad (16)$$

and

$$r_2(t) = -\frac{u}{16\sigma^5} \left\{ \begin{aligned} &c^4 u^4 (9 + 8\sigma^2 t^2) + \\ &2c^2 u^2 \omega^2 (-3 + 4\sigma^2 t^2) \\ &+ 2\omega^4 (-3 + \sigma^2 t^2) \end{aligned} \right\} \sin(\sigma t) \\ + \frac{3c^4 u^5}{16\sigma^5} \sin(5\sigma t) - \frac{3c^2 u^3 (c^2 u^2 - \omega^2)}{8\sigma^5} \sin(3\sigma t) + \\ \frac{3ut(c^2 u^2 - \omega^2)(4c^2 u^2 + \omega^2)}{8\sigma^4} \cos(\sigma t) - \\ \frac{3u^3 c^2 t (2c^2 u^2 + \omega^2)}{8\sigma^4} \cos(3\sigma t), \quad (17)$$

The approximate solution of Equation (2) may be written as:

$$r(t) = \lim_{\rho \rightarrow 1} (r_0(t) + \rho r_1(t) + \rho^2 r_2(t)). \quad (18)$$

Although the compact form of the solution of the equation of motion that is given by Equation (2) is rather difficult, we do not need to obtain an explicit form of the solution to study the long-time behavior. Actually, the unbounded solution comes from the presence of the secular terms that exist in the approximate solution as given in Equation (18). In fact, the previous traditional method does not enable us to remove these secular terms. It should be noted that the cancellation of the secular terms resulted in a trivial solution, which is not desired. As shown previously, the traditional perturbed solution in Equation (18) contains secular terms. So, one cannot theoretically judge the stability/instability of the system. As a result, the stability behavior will be obtained graphically through a set of figures. It is noteworthy that the HPM has been used for solving various kinds of nonlinear equations. Sometimes it is used to find the exact solution (El-Dib & Moatimid, 2018) or a closed approximate solution of the problem. (Ayati & Biazar, 2015) gave a brief elaboration on the convergence of the HPM.

#### 4. An approximate solution via the expanded frequency analysis

This study aims to achieve the stability profile of the problem. Unfortunately, the previous analysis does not enable us to do this. Therefore, another new technique

must be sought to achieve a periodic solution of the governing equation of motion that is given in Equation (2). In fact, this equation has a natural frequency. Thus, its zero-order solution becomes a periodic one.

Notice that the natural frequency of the problem is represented by the constant  $\sigma = \sqrt{2gc}$ . The following stability discussion is based on the expanded frequency analysis (see El-Dib & Moatimid, 2019). In accordance with this approach, a nonlinear frequency  $\Omega^2$  may be represented as follows:

$$\Omega^2 = \sigma^2 + \sum_{j=1}^{\infty} \rho^j \omega_j. \tag{19}$$

Inserting Equation (19) into Equation (2), one may write the homotopy equation as

$$\ddot{r} + \Omega^2 r + \rho [4c^2(r^2\ddot{r} + r\dot{r}^2) - (\omega^2 + \omega_1 + \rho\omega_2)r] = 0. \tag{20}$$

Taking the Laplace transform of Equation (20) and using the initial conditions that are given in Equation (3), one finds

$$L_T\{r(t; \rho)\} = \frac{u}{s^2 + \Omega^2} - \frac{1}{s^2 + \Omega^2} L_T\left\{\rho[4c^2(r^2\ddot{r} + r\dot{r}^2) - (\omega^2 + \omega_1 + \rho\omega_2)r]\right\}. \tag{21}$$

Employing the inverse transform of both sides of Equation (21), one obtains

$$r(t; \rho) = \frac{u}{\Omega} \sin(\Omega t) - L_T^{-1}\left[\frac{1}{s^2 + \Omega^2} L_T\left\{\rho[4c^2(r^2\ddot{r} + r\dot{r}^2) - (\omega^2 + \omega_1 + \rho\omega_2)r]\right\}\right] \tag{22}$$

Using the expansion of the dependent parameter  $r(t)$  from Equation (10), and then equating the coefficients of like powers of  $\rho$  on both sides, one gets

$$\rho^0 : r_0(t) = \frac{u}{\Omega} \sin(\Omega t), \tag{23}$$

$$\rho : r_1(t) = -L_T^{-1}\left[\frac{1}{s^2 + \Omega^2} L_T\left\{4c^2(r_0^2\ddot{r}_0 + r_0\dot{r}_0^2) - (\omega^2 + \omega_1)r_0\right\}\right], \tag{24}$$

and

$$\rho^2 : r_2(t) = -L_T^{-1}\left[\frac{1}{s^2 + \Omega^2} L_T\left\{\begin{aligned} &4c^2(r_0^2\ddot{r}_1 + 2r_0r_1\ddot{r}_0 + \\ &2r_0\dot{r}_0\dot{r}_1 + r_1\dot{r}_0^2) \\ &-(\omega^2 + \omega_1)r_1 - \omega_2r_0 \end{aligned}\right\}\right]. \tag{25}$$

Substituting from Equation (23) into Equation (24), one finds

$$r_1(t) = -L_T^{-1}\left[\frac{1}{s^2 + \Omega^2} L_T\left\{\begin{aligned} &-\frac{u(2c^2 + \omega^2 + \omega_1)}{\Omega} \sin(\Omega t) \\ &+ \frac{2c^2u^3}{\Omega} \sin(3\Omega t) \end{aligned}\right\}\right]. \tag{26}$$

The uniform valid expansion needs a cancellation of the secular terms. Therefore, the coefficient of the function  $\sin(\Omega t)$  must be canceled. This concept formulates the parameter  $\omega_1$  as follows:

$$\omega_1 = -(2c^2u^2 + \omega^2). \tag{27}$$

It follows that the periodic solution of  $r_1(t)$  becomes

$$r_1(t) = -\frac{c^2u^3}{\Omega^3} \sin^3(\Omega t). \tag{28}$$

Again, substituting from equations (23), (27) and (28) into Equation (26), one finds

$$r_2(t) = -L_T^{-1}\left[\frac{1}{s^2 + \Omega^2} L_T\left\{\begin{aligned} &\frac{u(9c^4u^4 - 2\Omega^2\omega_2)}{2\Omega^3} \sin(\Omega t) \\ &-\frac{9c^4u^5}{2\Omega^3} (2\sin(3\Omega t) - \sin(5\Omega t)) \end{aligned}\right\}\right]. \tag{29}$$

Again, the cancellation of the secular term requires

$$\omega_2 = \frac{9c^4u^4}{2\Omega^2}. \tag{30}$$

Therefore, the direct calculations in Equation (29) gives

$$r_2(t) = \frac{3c^4u^5}{4\Omega^5} (3 - 2\cos(2\Omega t)) \sin^3(\Omega t). \tag{31}$$

As previously shown in the limiting of Equation (18), the approximate periodic solution of the equation of motion that is given in Equation (2) may be written as follows:

$$r(t) = \frac{u}{\Omega} \sin(\Omega t) - \frac{c^2u^3}{\Omega^3} \sin^3(\Omega t) + \frac{3c^4u^5}{4\Omega^5} (3 - 2\cos(2\Omega t)) \sin^3(\Omega t). \tag{32}$$

Actually, the approximate solution in Equation (32) requires that the arguments of the trigonometric functions must be real values. For this purpose, we return back to Equation (19). Substituting Equations (27) and (30) into Equation (19), the following characteristic equation is obtained:

$$\Omega^4 + (\omega^2 + 2c^2u^2 - 2gc)\Omega^2 - \frac{9}{2}c^4u^4 = 0. \tag{33}$$

Equation (33) is an algebraic quartic equation in  $\Omega$ . It is convenient to solve this equation by means of the HPM as follows:

The homotopy equation in this case becomes

$$\Omega^2 = \frac{9c^4u^4}{2\Gamma^2} - \varepsilon \frac{\Omega^4}{\Gamma^2}, \tag{34}$$

where  $\Gamma = \sqrt{\omega^2 + 2c^2u^2 - 2gc}$ , and  $\varepsilon \in [0,1]$  is a new artificial homotopy parameter.

As usual, the frequency  $\Omega$  is expanded as given in Equation (10). Using similar arguments as before, one gets:

$$\Omega = \Omega_0 - \frac{\Omega_0^3}{2\Gamma^2} + \frac{7\Omega_0^5}{8\Gamma^4}, \quad (35)$$

$$\text{where } \Omega_0 = \frac{3c^2u^2}{\Gamma\sqrt{2}}.$$

In order for  $\Omega$  to be of real values, we must have the following stability criterion:

$$\omega > \sqrt{2gc - 2c^2u^2}. \quad (36)$$

The effects of the characteristic parameters of the problem in the stability profile will be discussed through the numerical calculations in Section 6.

## 5. External excitation via an influence of an oscillating vertical gravity

Here the external excitation of the problem at hand is analyzed. The excitation appears as a variable (i.e., time-dependent) coefficient in the governing equations of motion. This excitation may occur due to an oscillating gravitational force. In accordance with this concept, consider a gravitational force in the form of  $(g_0 - g_1 \cos(2\omega t))$ . In this case, the equation of motion that is given by Equation (2) may be written as a transcendental cubic nonlinear Mathieu equation as:

$$\ddot{r}(1 + 4c^2r^2) + 4c^2r\dot{r}^2 + \theta^2r - 2\kappa^2 \cos(2\omega t)r - \omega^2r = 0, \quad (37)$$

where  $\theta^2 = 2cg_0$ , and  $\kappa^2 = cg_1$ .

According to the HPM, the homotopy equation may be formulated as follows:

$$\ddot{r} + \theta^2r + \rho[4c^2(r^2\ddot{r} + r\dot{r}^2) - (\omega^2 + 2\kappa^2 \cos(2\omega t))r] = 0. \quad (38)$$

In order to analyze the external excitation, through the current case, the multiple time-scales technique is adapted. Therefore, uniform valid expansion of Equation (37) may be viewed as a function of three independent variables rather than one parameter (time). In light of the He-multiple scale method (El-Dib 2017), one may regard the dependent variable to be a function of  $t$ ,  $\rho t$  and  $\rho^2 t$ . The underlying idea of the method of multiple-time scales is to consider the expansion that represents the response as a function of multiple independent variables, or scales, instead of a single variable. The method of multiple-time scales, through a little more involved, has advantages over the Lindstedt-Poincaré method.

The first step is to introduce new independent variables according to

$$T_n = \rho^n t, \quad n = 0, 1, 2, \dots \quad (39)$$

It follows that the derivatives w.r.t the time-independent variables become expansions in terms of the partial derivatives as follows:

$$\begin{aligned} \frac{d}{dt} &\equiv \frac{dT_0}{dt} \frac{\partial}{\partial T_0} + \frac{dT_1}{dt} \frac{\partial}{\partial T_1} + \frac{dT_2}{dt} \frac{\partial}{\partial T_2} + \dots \\ &= D_0 + \rho D_1 + \rho^2 D_2 + \dots \end{aligned} \quad (40)$$

and

$$\frac{d^2}{dt^2} \equiv D_0^2 + 2\rho D_0 D_1 + \rho^2 (D_1^2 + 2D_0 D_2) + \dots \quad (41)$$

One may assume that the solution of Equation (38) may be represented as an expansion having the following form:

$$\begin{aligned} r(t; \rho) &= r_0(T_0, T_1, T_2, \dots) + \rho r_1(T_0, T_1, T_2, \dots) \\ &\quad + \rho^2 r_2(T_0, T_1, T_2, \dots) + \dots \end{aligned} \quad (42)$$

It should be noted that the number of the needed independent time scales depend on the order at which the expansion is carried out. Namely, if the expansion is carried to  $O(\rho^2)$ , then  $T_0$  and  $T_1$  are only needed. For convenience, to obtain a more accurate expansion, we carry out the expansion up to  $O(\rho^3)$ . Therefore, three-time scales ( $T_0, T_1$  and  $T_2$ ) are utilized. Substituting from equations (39-42) into Equation (38), and then equating the coefficient of like powers of  $\rho$ , one finds the following equations:

$$\rho^0 : (D_0^2 + \theta^2)r_0 = 0, \quad (43)$$

$$\begin{aligned} \rho : (D_0^2 + \theta^2)r_1 &= -2D_0 D_1 r_0 - 4c^2 [r_0^2 D_0^2 r_0 + r_0 (D_0 r_0)^2] \\ &\quad + [\omega^2 + \kappa^2 (e^{2i\omega T_0} + e^{-2i\omega T_0})] r_0, \end{aligned} \quad (44)$$

and

$$\begin{aligned} \rho^2 : (D_0^2 + \theta^2)r_2 &= -2D_0 D_1 r_1 - (D_1^2 r_0 + 2D_0 D_2 r_2) \\ &\quad - 4c^2 \left[ r_0^2 (2D_0 D_1 r_0 + D_0^2 r_1) + 2r_0 r_1 D_0^2 r_0 + \right. \\ &\quad \left. 2r_0 D_0 r_0 (D_1 r_0 + D_0 r_1) + r_1 (D_0 r_0)^2 \right] \\ &\quad + [\omega^2 + \kappa^2 (e^{2i\omega T_0} + e^{-2i\omega T_0})] r_1 \end{aligned} \quad (45)$$

With this approach, it is convenient to write the solution of Equation (45) in the following form:

$$r_0 = A(T_1, T_2) e^{i\theta T_0} + c.c., \quad (46)$$

where  $A$  is an unknown complex function and  $c.c.$  represents the complex conjugate of the preceding terms.

The governing equations of the complex function  $A$  are obtained by requiring the distribution functions  $r_1$  and  $r_2$  to be of a periodic nature.

Substituting Equation (46) into Equation (44) leads to

$$\begin{aligned} (D_0^2 + \theta^2)r_1 = & 8c^2\theta^2 A^3 e^{3i\theta T_0} + \\ & \kappa^2 \left( A e^{i(\theta+2\varpi)T_0} + A e^{i(\theta-2\varpi)T_0} \right) + \\ & \left( -2i\theta D_1 A + 8c^2\theta^2 A^2 \bar{A} + \omega^2 A \right) e^{i\theta T_0} + c.c., \end{aligned} \quad (47)$$

here, the complex function  $\bar{A}$  represents the complex conjugate of the complex function  $A$ .

The required uniform valid expansion of the function  $r_1$  needs elimination of the secular terms. These secular terms are the coefficient of the exponentials  $e^{i\theta T_0}$  and  $e^{-i\theta T_0}$ . Therefore, the uniform valid expansion requires

$$-2i\theta D_1 A + 8c^2\theta^2 A^2 \bar{A} + \omega^2 A = 0. \quad (48)$$

Equation (48) is well-known as the solvability condition. Sometimes, it is called the amplitude equation. It follows that the particular solution of Equation (47) may be written as

$$r_1 = -c^2 A^3 e^{3i\theta T_0} - \frac{A\kappa^2}{4\varpi(\theta+\varpi)} e^{i(\theta+2\varpi)T_0} + \frac{A\kappa^2}{4\varpi(\theta-\varpi)} e^{i(\theta-2\varpi)T_0} + c.c. \quad (49)$$

Substituting from equations (46), (48) and (49) into Equation (45), after lengthy but straightforward calculations, one finds the following equations:

$$\begin{aligned} (D_0^2 + \theta^2)r_2 = & -72c^4\theta^2 A^5 e^{5i\theta T_0} - 72c^4\theta^2 A^4 \bar{A} e^{3i\theta T_0} \\ & - \frac{(6\theta^2 + 9\theta\varpi + 5\varpi^2)c^2\kappa^2 A^3 e^{i(3\theta+2\varpi)T_0}}{\varpi(\theta+\varpi)} + \frac{A\kappa^4 e^{i(\theta-4\varpi)T_0}}{4\varpi(\theta-\varpi)} \\ & + \kappa^2 \left( \frac{\omega^2 A}{2\theta(\theta-\varpi)} + \frac{12\varpi^2 c^2 A^2 \bar{A}}{(\theta^2 - \varpi^2)} \right) e^{i(\theta-2\varpi)T_0} \\ & - \frac{A\kappa^4 e^{i(\theta+4\varpi)T_0}}{4\varpi(\theta+\varpi)} + \kappa^2 \left( \frac{\omega^2 A}{2\theta(\theta+\varpi)} + \frac{12\varpi^2 c^2 A^2 \bar{A}}{(\theta^2 - \varpi^2)} \right) e^{i(\theta-2\varpi)T_0} \\ & + \frac{(6\theta^2 - 9\theta\varpi + 5\varpi^2)c^2\kappa^2 A^3 e^{i(3\theta-2\varpi)T_0}}{\varpi(\theta-\varpi)} + \\ & + \left( \begin{aligned} & -2i\theta D_2 A - 72\theta^2 c^4 A^3 \bar{A}^2 - 4c^2\omega^2 A^2 \bar{A} \\ & + \frac{\omega^4 A}{4\theta^2} + \frac{\kappa^4 A}{2(\theta^2 - \varpi^2)} \end{aligned} \right) e^{i\theta T_0} + c.c. \end{aligned} \quad (50)$$

To eliminate the secular terms from Equation (50), we must have

$$-2i\theta D_2 A - 72\theta^2 c^4 A^3 \bar{A}^2 - 4c^2\omega^2 A^2 \bar{A} + \frac{\omega^4 A}{4\theta^2} + \frac{\kappa^4 A}{2(\theta^2 - \varpi^2)} = 0. \quad (51)$$

It follows that the periodic solution of Equation (50) may be written as

$$\begin{aligned} r_2 = & \frac{18}{31} c^4 \theta^2 A^5 e^{5i\theta T_0} + 9c^4 \theta^2 A^4 \bar{A} e^{3i\theta T_0} \\ & + \frac{(6\theta^2 + 9\theta\varpi + 5\varpi^2)c^2\kappa^2 A^3 e^{i(3\theta+2\varpi)T_0}}{4\varpi(\theta+\varpi)^2(2\theta+\varpi)} + \frac{A\kappa^4 e^{i(\theta-4\varpi)T_0}}{4\varpi(\theta-\varpi)} + \\ & \kappa^2 \left( \frac{\omega^2 A}{8\theta\varpi(\theta-\varpi)^2} + \frac{12\varpi c^2 A^2 \bar{A}}{4(\theta+\varpi)(\theta-\varpi)^2} \right) e^{i(\theta-2\varpi)T_0} \\ & + \frac{A\kappa^4 e^{i(\theta+4\varpi)T_0}}{8\varpi^2(\theta+\varpi)(\theta+2\varpi)} + \\ & \kappa^2 \left( \frac{\omega^2 A}{8\theta\varpi(\theta^2 - \varpi^2)} + \frac{12\varpi c^2 A^2 \bar{A}}{4(\theta+\varpi)(\theta-\varpi)^2} \right) e^{i(\theta+2\varpi)T_0} \\ & - \frac{(6\theta^2 - 9\theta\varpi + 5\varpi^2)c^2\kappa^2 A^3 e^{i(3\theta-2\varpi)T_0}}{4(\theta-\varpi)^2(2\theta-\varpi)} + c.c. \end{aligned} \quad (52)$$

### 5.1 Stability analysis in the non-resonance case

To investigate the stability analysis, throughout the non-resonance case, we return to the amplitude equations that are given by equations (48) and (50). In fact, these equations enable us to determine the unknown function  $A$  in terms of the time-independent variables  $T_1$  and  $T_2$ . In addition, the stability behavior mainly depends on the solutions of these equations. For this purpose, integrate Equation (48) partially *w.r.t.* the variable  $T_1$ . Then integrate Equation (50) partially *w.r.t.* the variable  $T_2$ . In other words, equations (48) and (50) are simply multiplied by  $\rho$  and  $\rho^2$ , respectively. It follows that the partial differentiations in these amplitude equations may be transformed into  $\frac{dA}{dt}$ . Finally, one may obtain the following amplitude equation:

$$\frac{dA}{dt} = i \left[ \begin{aligned} & -36c^4\theta A^3 \bar{A}^2 + \frac{2c^2}{\theta}(2\theta^2 - \omega^2)A^2 \bar{A} \\ & + \frac{(2\theta^2\kappa^4 + 4\theta^4\omega^2 - 4\theta^2\varpi^2\omega^2 + \theta^2\omega^4 - \varpi^2\omega^4)}{8\theta^3(\theta^2 - \varpi^2)} A \end{aligned} \right]. \quad (53)$$

Equation (53) is a first-order nonlinear differential equation with an imaginary coefficient. It is similar to the well-known Landau equation. This amplitude equation will govern the stability criterion of the problem. The solution of this equation may be obtained by utilizing the polar form formula as given below:

The solution of Equation (53) has the form

$$A = \alpha(t) \text{Exp}(i\beta(t)), \quad (54)$$

where the functions  $\alpha(t)$  and  $\beta(t)$  are two real functions on the time.

Substituting Equation (54) into Equation (53), and then equating the real and imaginary parts on the two sides, one gets the following solutions:

$$\alpha = \alpha_0, \quad (55a)$$

and

$$\beta = \left[ \begin{array}{l} -36c^4\theta\alpha_0^4 + \frac{2c^2}{\theta}(2\theta^2 - \omega^2)\alpha_0^2 \\ + \frac{(2\theta^2\kappa^4 + 4\theta^4\omega^2 - 4\theta^2\omega^2\omega^2 + \theta^2\omega^4 - \omega^2\omega^4)}{8\theta^3(\theta^2 - \omega^2)} \end{array} \right] t + \beta_0 \quad (55b)$$

where  $\alpha_0$  and  $\beta_0$  are the two real integration constants.

Actually, all the parameters of the problem, except the initial velocity  $u$ , are included throughout the solution of the amplitude equation. Unfortunately, the solutions that are given in equations (55a) and (55b) indicate that the system **is always stable**. Hence, to achieve the stability criteria, we will proceed to investigate the resonance cases. Therefore, the following subsection is depicted to discuss the resonance cases.

The approximate solution, in the non-resonant case, may be formulated as follows:

$$r(t) = \lim_{\rho \rightarrow 1} (r_0(t) + \rho r_1(t) + \rho^2 r_2(t)), \quad (56)$$

where  $r_0$ ,  $r_1$  and  $r_2$  are given in equations (46), (49) and (51), respectively. In addition, Equation (53) must be included.

## 5.2 Stability analysis in the resonance cases

As seen in the previous subsection, the non-resonance case fails to achieve the stability criteria. Consequently, the following discussion focuses on the resonance cases. It should be noted that resonance occurs when  $\kappa$  is large, or when the frequency of the external excited gravitational force  $\varpi$  is nearer to the resonance of the system. This means that the system will oscillate with a high amplitude. Generally, in a mechanical system, it is better to avoid resonance caused by a small driving force that can cause large amplitude vibration and could subsequently damage the system. In the case when the frequency of the excited force is nearer to the natural frequency of the system,  $\varpi \approx \theta$ , the oscillation is defined as a primary or main resonance. It should be noted that if  $\varpi \approx \theta/2$ , the resonance is called super-harmonic resonance. On the other hand, if  $\varpi \approx 2\theta$

the resonance is termed as sub-harmonic resonance. In fact, there are several powers in the different stages, as shown in equations (53) and (55). It follows that there are many resonance cases.

To avoid lengthy calculations, the present analysis is only concerned with one of these resonance cases. For this purpose, instead of the frequency of the external excitation  $\varpi$ , one may introduce a detuning parameter  $\delta$ , that quantitatively describes the nearness of  $\varpi$  to  $\theta/2$ . This helps one to recognize the terms in the governing equation for  $r_2$  that lead to secular, and nearly secular (small divisor), terms. Accordingly, one may write

$$\varpi = \frac{1}{2}\theta + \frac{1}{2}\delta\rho. \quad (57)$$

In this case, one obtains

$$-i(\theta - 4\varpi)T_0 = i\theta T_0 + 2i\delta T_1. \quad (58)$$

In this case, there is no contribution in the secular that appears in Equation (45). It follows that the amplitude equation that is given in equation (48) is unaffected. On the other hand, the governing equation of  $r_2$  has an additional secular term. Inserting Equation (58) into Equation (50), one gets

$$\begin{aligned} (D_0^2 + \theta^2)r_2 = & -72c^4\theta^2 A^5 e^{5i\theta T_0} - 72c^4\theta^2 A^4 \bar{A} e^{3i\theta T_0} \\ & - \frac{(6\theta^2 + 9\theta\varpi + 5\varpi^2)c^2\kappa^2 A^3 e^{i(3\theta+2\varpi)T_0}}{\varpi(\theta+\varpi)} \\ & + \kappa^2 \left( \frac{\omega^2 A}{2\theta(\theta-\varpi)} + \frac{(5\theta^3 - \theta^2\varpi - 4\theta\varpi^2 + 12\varpi^3)c^2 A^2 \bar{A}}{\varpi(\theta^2 - \varpi^2)} \right) e^{i(\theta-2\varpi)T_0} \\ & - \frac{A\kappa^4 e^{i(\theta+4\varpi)T_0}}{4\varpi(\theta+\varpi)} + \kappa^2 \left( \frac{\omega^2 A}{2\theta(\theta+\varpi)} + \frac{(5\theta^3 + \theta^2\varpi - 4\theta\varpi^2 - 12\varpi^3)c^2 A^2 \bar{A}}{\varpi(\theta^2 - \varpi^2)} \right) \\ & e^{i(\theta-2\varpi)T_0} + \frac{(6\theta^2 - 9\theta\varpi + 5\varpi^2)c^2\kappa^2 A^3 e^{i(3\theta-2\varpi)T_0}}{\varpi(\theta-\varpi)} + \\ & + \left( \begin{array}{l} -2i\theta D_2 A - 72\theta^2 c^4 A^3 \bar{A}^2 - 4c^2 \omega^2 A^2 \bar{A} + \frac{\omega^4 A}{4\theta^2} \\ + \frac{\kappa^4 A}{2(\theta^2 - \varpi^2)} + \frac{\bar{A}\kappa^4 e^{2i\delta T_1}}{4\varpi(\theta - \varpi)} \end{array} \right) e^{i\theta T_0} + c.c.. \end{aligned} \quad (59)$$

The elimination of the secular term from Equation (59) leads to

$$\begin{aligned} -2i\theta D_2 A - 72c^4\theta^2 A^3 \bar{A}^2 - 4c^2 \omega^2 A^2 \bar{A} + \frac{\omega^4 A}{4\theta^2} \\ + \frac{\kappa^4 A}{2(\theta^2 - \varpi^2)} + \frac{\bar{A}\kappa^4 e^{2i\delta T_1}}{4\varpi(\theta - \varpi)} = 0. \end{aligned} \quad (60)$$

It follows that the particular solution of Equation (59) becomes

$$\begin{aligned}
 r_2 = & \frac{18}{31}c^4\theta^2A^5e^{5i\theta T_0} + 9c^4\theta^2A^4\bar{A}e^{3i\theta T_0} \\
 & + \frac{(6\theta^2 + 9\theta\varpi + 5\varpi^2)c^2\kappa^2A^3e^{i(3\theta+2\varpi)T_0}}{4\varpi(\theta+\varpi)^2(2\theta+\varpi)} + \\
 & \kappa^2 \left( \frac{\omega^2 A}{8\theta\varpi(\theta-\varpi)^2} + \frac{(5\theta^3 - \theta^2\varpi - 4\theta\varpi^2 + 12\varpi^3)c^2A^2\bar{A}}{4\varpi^2(\theta+\varpi)(\theta-\varpi)^2} \right) e^{i(\theta-2\varpi)T_0} \\
 & + \kappa^2 \left( \frac{\omega^2 A}{8\theta\varpi(\theta^2-\varpi^2)} + \frac{(5\theta^3 + \theta^2\varpi - 4\theta\varpi^2 - 12\varpi^3)c^2A^2\bar{A}}{4\varpi^2(\theta+\varpi)(\theta-\varpi)^2} \right) e^{i(\theta+2\varpi)T_0} \\
 & + \frac{A\kappa^4 e^{i(\theta+4\varpi)T_0}}{8\varpi^2(\theta+\varpi)(\theta+2\varpi)} \\
 & - \frac{(6\theta^2 - 9\theta\varpi + 5\varpi^2)c^2\kappa^2A^3e^{i(3\theta-2\varpi)T_0}}{4(\theta-\varpi)^2(2\theta-\varpi)} + c.c. \quad (61)
 \end{aligned}$$

Finally, the approximate solution for instances of the resonance case is given in Equation (56). Keep in mind that the functions  $r_0$ ,  $r_1$  and  $r_2$  are given in equations (46), (49) and (61), respectively. In addition, the unknown function  $A(t)$  may be obtained as follows:

Using similar arguments as that is shown in the non-resonance case, one gets

$$\frac{dA}{dt} = i \left[ a A^3 \bar{A}^2 + b A^2 \bar{A} - d A - e \bar{A} e^{2i\delta t} \right], \quad (62)$$

where

$$\begin{aligned}
 a = & -36c^4\theta, \quad b = \frac{2c^2}{\theta}(2\theta^2 - \omega^2), \\
 d = & -\frac{(2\theta^2\kappa^4 + 4\theta^4\omega^2 - 4\theta^2\varpi^2\omega^2 + \theta^2\omega^4 - \varpi^2\omega^4)}{8\theta^3(\theta^2 - \varpi^2)}
 \end{aligned}$$

$$\text{and } e = \frac{\kappa^4}{8\theta\varpi(\theta-\varpi)}.$$

Equation (62) is a first-order nonlinear differential equation with complex and variable coefficients. Its solution may be obtained by the following transformation:

$$A(t) = B(t)e^{i\delta t}, \quad (63)$$

where  $B(t)$  must be real and time-dependent functions.

Substituting from Equation (63) into Equation (62), and then separating the real and imaginary parts, one gets:

$B(t) = B_0$ , where  $B_0 \neq 0$  is a real parameter. This parameter satisfies the following relation:

$$aB_0^4 + bB_0^2 - (d + e + \delta) = 0. \quad (64)$$

Equation (64) may be analyzed in the same manner used in Equation (33). In the present case, we seek only that condition which makes  $B_0$  be of real values.

Because of the nature of  $B_0$ , one finds

$$d + e + \delta < 0. \quad (65)$$

Inserting the stability criterion as given in Equation (65) into the transition curve that is represented in Equation (57), one finds the final stability condition in the non-resonant case as:

$$2\varpi - \theta + d + e > 0. \quad (66)$$

Actually, the transition curve that separates the stable from the unstable regions is described by the following equation:

$$2\varpi - \theta + d + e = 0. \quad (67)$$

In fact, Equation (67) is a transcendental equation. It includes all the parameters of the considered problem except for the initial velocity  $u$ . It is convenient to graph this equation by means of the Mathematica software to show the influence of some parameters in the stability diagram. It is more convenient to discuss the stability profile using another simple technique. Therefore, in the next Section, the linearization technique to check the stability of the linearized equation is utilized.

## 6. The linearization technique

In the following linearization technique, the linear system is used to approximate the behavior of the nonlinear system. The analysis is classified into two categories (see 6.1 and 6.2).

### 6.1 The autonomous system

This is concerned with the governing equation as given by Equation (2) in which the gravitational force is only uniform. The stability analysis, in this case, corresponds to the occurrence of the non-resonance case as given in the previous analysis. For this purpose, consider the following transformations:

$$r = x, \text{ and } \dot{r} = y. \quad (68)$$

It follows that the governing equation given by Equation (2) may be represented by the following first-order nonlinear equations:

$$\dot{x} = f(x, y), \text{ and } \dot{y} = h(x, y), \quad (69)$$

where

$$f(x, y) = y, \alpha^2 = 2gc - \omega^2, \text{ and } h(x, y) = -\frac{4c^2xy^2}{1+4c^2x^2} - \frac{\alpha^2x}{1+4c^2x^2}.$$

The constant solutions of this system are called the equilibria. They satisfy the following equations:

$$f(x_0, y_0) = 0, \text{ and } h(x_0, y_0) = 0. \quad (70)$$

The equilibrium solution of equations (70) is exactly the origin (critical point).

Now, using the Taylor expansion to expand the functions  $f(x, y)$  and  $h(x, y)$  around the critical point, considering only the linear terms, one finds the following Jacobian matrix:

$$J = \begin{pmatrix} 0 & 1 \\ -\frac{(1-4c^2x^2)(\alpha+4c^2y^2)}{(1+4c^2x^2)^2} & -\frac{8c^2xy}{1+4c^2x^2} \end{pmatrix}. \quad (71)$$

At the origin, the Jacobian matrix becomes

$$J_0 = \begin{pmatrix} 0 & 1 \\ -\alpha^2 & 0 \end{pmatrix}. \quad (72)$$

The above matrix has the eigenvalues:

$$\lambda = \pm i\alpha. \quad (73)$$

If  $2gc - \omega^2 > 0$ , it follows that  $\alpha$  becomes of real values, and the type of the critical point is a center. The behavior of the system is stable, but not asymptotically stable. In contrast, if  $2gc - \omega^2 < 0$ , it follows that  $\alpha$  is pure imaginary, and the type of the critical point is a saddle. In this case, the system has an instability behavior.

The previous analysis may be simplified as follows:

Returning to the governing equation as given in Equation (2), it is evident that the trivial solution ( $r = 0$ ) satisfies this equation. Therefore, the linear solution of the equation of motion may be obtained around this zero-order solution. For this purpose, one may assume the linear solution as

$$r = 0 + \eta, \quad (74)$$

Substituting from Equation (74) into Equation (2), and then considering only the linearized term, one finds

$$\ddot{\eta} + \alpha^2 = 0. \quad (75)$$

It follows that the system is stable if  $\alpha$  has real. Otherwise, the system has an unstable behavior. The comparison with the obtained results as given in the subsection 5.1

shows that the present analysis is more accurate than the previous one.

## 6.2 The non-autonomous system

This subsection analyzes the governing equation that is given in Equation (2), in the case of the excited gravitational force. The stability analysis, in this case, corresponds to the resonance given throughout the multiple time-scale technique.

For simplicity, following similar arguments as before, one may write

$$r = 0 + \zeta, \quad (76)$$

It follows that the excited equation of motion becomes

$$\ddot{\zeta} + (\alpha^2 - 2\kappa^2 \cos(2\omega t))\zeta = 0. \quad (77)$$

Now, normalizing the time  $t$ , such that  $t = \frac{\tau}{\omega}$ , it follows that Equation (77) becomes

$$\zeta'' + (P - S \cos(2\tau))\zeta = 0, \quad (78)$$

where the prime refers to differentiation with respect to the new parameter  $\tau$ ,  $P = \frac{\alpha^2}{\omega^2}$ , and  $S = \frac{2\kappa^2}{\omega^2}$ .

Equation (78) is a standard Mathieu equation. This equation has been studied extensively. It appears in many problems in applied mathematics, such as with the instability of a transverse column subjected to an excited periodic load and to electromagnetic wave propagation in a medium with periodic forces.

The stability of this equation has been extensively studied by Nayfeh (1973) as well as Nayfeh and Mook (1979). According to Floquet theory (Neves 2009), the transition curves, in the  $(P-S)$  plane, separate the stable from unstable regions. In addition, the regions between these curves are unstable. In contrast, the regions outside these curves are stable.

In accordance with the HPM, these transition curves may be obtained as follows:

The homotopy equation may be written as

$$\zeta'' + (P - \rho S \cos(2\tau))\zeta = 0, \rho \in [0, 1]. \quad (79)$$

Expanding the parameters  $\zeta$  and  $P$  as

$$\zeta(\tau; \rho) = \zeta_0 + \rho\zeta_1 + \rho^2\zeta_2 + \dots, \quad (80)$$

$$P = n^2 + \rho P_1 + \rho^2 P_2 + \dots \quad n = 0, 1, 2, \dots \quad (81)$$

Substituting from equations (80) and (81) into Equation (79), one finds the zero-order solution

$$\zeta_0 = \{\sin(n\tau), \cos(n\tau)\}. \quad (82)$$

Following similar arguments given earlier by Moatimid and Obied Allah (2010), one gets the following transition curves:

In the case of  $n=0$ :

$$P = -\frac{S^2}{8} + O(\rho^4), \quad (83)$$

In the case of  $n=1$ :

$$P = 1 \pm \frac{S}{2} - \frac{S^2}{32} - \frac{S^3}{512} + O(\rho^4), \quad (84)$$

In the case of  $n=2$ :

$$P = 4 - \frac{S^2}{48} + O(\rho^4). \quad (85)$$

As seen in the resonance case, throughout the analysis of the multiple time-scales method, there exists a finite number of the transition curve. The previous analysis obtains only one of them. In contrast, in the present case there are many transition curves. One can conclude that the analysis in the linearization techniques of stability is richer than the previous one.

## 7. Numerical calculations

In order to estimate the previous theoretical outcomes, numerical calculations are needed. Therefore, in what follows, numerical investigations are made to illustrate the effects of the various parameters as well as the obtained solutions in a stability picture.

### 7.1 An investigation of the approximate solution given by Equation (18).

The approximate solution that is given by Equation (18) depicts the behavior of the distribution function versus the time. Furthermore, the influences of the various governed parameters on the distribution function are plotted. Therefore, the following figures are displayed. Figure 2 plotted the approximate solution of  $r(t)$  versus the time  $t$ . As previously shown, the presence of the secular term prevents the oscillatory solution to appear. For small values of time as  $t \in [0,10]$ , the solution seems to be stable. For large values of time, the amplitudes of the solution are elongated. Figure 3 indicates the influence of the angular velocity of the parabola. It is evident that an interval of the time is taken to display the required influence, where

$t \in [40,50]$ . The increase in the frequency  $\omega$  accelerates the amplitude of the solution. This means that the parameter  $\omega$  has a destabilizing influence. Actually, this is of physical significance. The influence of the initial linear velocity  $u$  of the approximate solution is shown in Figure 4. As in Figure 3, a time interval is considered at which the influence of the variation of  $u$  is seen, where  $t \in [40,50]$ . Furthermore, as previously mentioned, the initial linear velocity has a destabilizing influence. Finally, Fig. 5 shows the effect of the parameter  $c$ . It can be seen that the amplitude of the solution increases with the decrease of this parameter. In addition, the wavelength decreases with the increase of parameter  $c$ . In other words, the first two zeros on the horizontal  $t$ -axis shift in the direction of  $t$  as the parameter is increased. These observations show that this parameter has a stabilizing effect.

### 7.2 An investigation of the approximate solution given by Equation (32)

As previously shown, the cancellation of the secular term produces an approximate periodic solution. Now, it is convenient to give the periodic solution from Equation (32). In addition, we focus on the influence of the physical parameters of the problem. Fig. 6 gives the distribution function  $r(t)$  versus the time  $t$ . Actually, the stability condition that is given in Equation (36) must be verified. The artificial frequency is real and of value  $\Omega = 0.016 \text{ rad/sec}$  (see Figure 6 caption). This figure indicates the periodic nature of the distribution function  $r(t)$  versus time. The influence of the various physical parameters in the periodic approximate solution as given in Equation (32) are shown in the following figures. The effect of the angular velocity  $\omega$  in the approximate periodic solution is depicted in Figure 7. The amplitude of the approximate solution increases when the initial velocity increased. This indicates a destabilizing influence of this parameter. The same mechanism was first observed in the previous case by Equation (18). The influence of the initial velocity of the periodic solution is depicted in Figure 8. Here, one can see that the amplitude of the wave solution decreases as the initial velocity increases. Thus, the increase in the initial velocity plays a stabilizing effect. This is in contrast to the previous case. Figure 9 shows the influence of parameter  $c$ , which measures the reciprocal of the length of the latus rectum of the parabola. It is evident that the amplitude of the wave solution decreases as the value increased. These observations show a stabilizing influence for parameter  $c$ . This influence is in agreement with the previous case.

### 7.3 An investigation of the stability analysis of the parametric excitation given by Equation (67)

In the above two cases, the approximate solutions were obtained and graphed. In order to avoid repeating the graphs of the approximate solutions, other graphs were plotted to illustrate the stability criterion for the parametric resonance case. Thus, the stability picture depicts the transition that is obtained by Equation (67). This equation seems to be a single transition curve. Actually, it represents a transcendental equation as  $f(\varpi, \omega) = 0$ . Mathematica software was used to graph this equation. As shown from the Floquet theorem (Neves, 2009), the regions between the transition curves are unstable and vice-versa outside these curves. For this purpose, Figure 10 indicates the influence of the coefficient of the existing force  $g_1$  in the stability picture. The figure shows that an increase in this parameter causes a stabilizing influence. This is in contrast when there is an absence of external excitation. The effect of the excitation parameter  $g_1$  is shown in Figure 11. In contrast to the previous mechanism, for large values of  $c$ , the unstable regions increased. This shows that this parameter has a destabilizing effect.

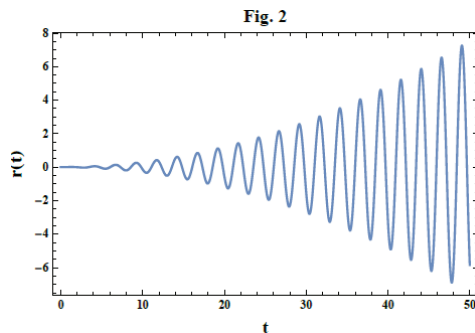


**Fig. 2.** Depicts the approximate solution that is given in Equation (22) for a system having the particulars:  $g = 32 \text{ ft/sec}^2$ ,  $c = 0.1 \text{ ft}^{-1}$ ,  $u = 0.01 \text{ ft/sec}$ , and  $\omega = 2.5 \text{ rad/sec}$ .

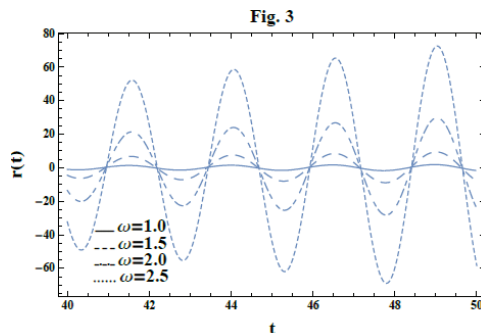


**Fig. 3.** Depicts the approximate solution that is given in Equation (22) for a system having the particulars:  $g = 32 \text{ ft/sec}^2$ ,  $c = 0.1 \text{ ft}^{-1}$ ,  $u = 0.1 \text{ ft/sec}$  with the variation of the frequency  $\omega$ .

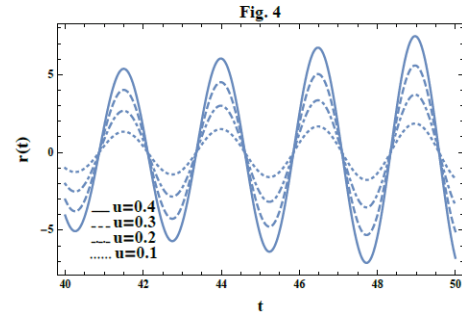


**Fig. 4.** Depicts the approximate solution that is given in Equation (22) for a system having the particulars:  $g = 32 \text{ ft/sec}^2$ ,  $c = 0.1 \text{ ft}^{-1}$ ,  $\omega = 1.0 \text{ rad/sec}$ .

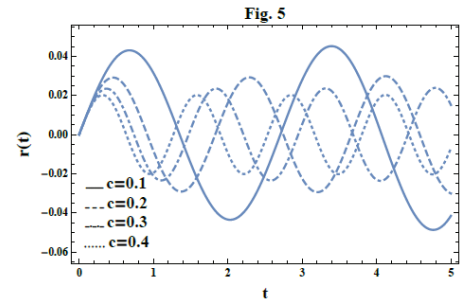


**Fig. 5.** Depicts the approximate solution that is given in Equation (22) for a system having the particulars:  $g = 32 \text{ ft/sec}^2$ ,  $c = 0.1 \text{ ft}^{-1}$ ,  $\omega = 1.0 \text{ rad/sec}$  with the variation of the reciprocal of the latus rectum  $c$ .

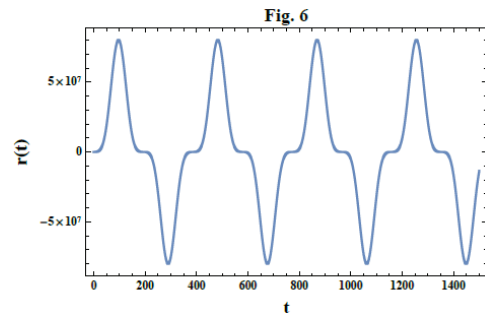


**Fig. 6.** Depicts the approximate solution that is given in Equation (36) for a system having the particulars:  $g = 32 \text{ ft/sec}^2$ ,  $c = 0.1 \text{ ft}^{-1}$ ,  $\omega = 12 \text{ rad/sec}$ ,  $u = 3.0 \text{ ft/sec}$ , and  $\Omega = 0.016 \text{ rad/sec}$ .

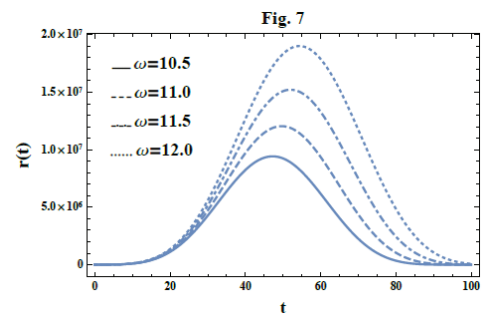


**Fig. 7.** Depicts the approximate solution that is given in Equation (36) for a system having the particulars:  $g = 32 \text{ ft/sec}^2$ ,  $c = 0.1 \text{ ft}^{-1}$ ,  $u = 4.0 \text{ ft/sec}$  with the variation of the angular frequency  $\omega$ .

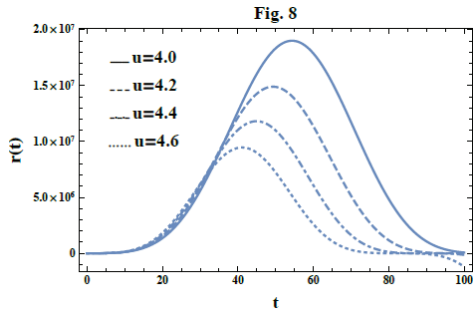


**Fig. 8.** Depicts the approximate solution that is given in Equation (36) for a system having the particulars:  $g = 32 \text{ ft/sec}^2$ ,  $c = 0.1 \text{ ft}^{-1}$ ,  $\omega = 12 \text{ rad/sec}$  with the variation of the initial velocity  $u$ .

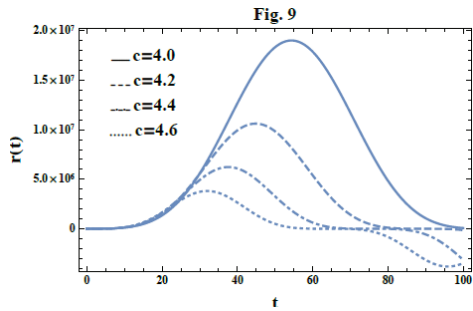


**Fig. 9.** Depicts the approximate solution that is given in Equation (36) for a system having the particulars:  $g = 32 \text{ ft/sec}^2$ ,  $c = 0.1 \text{ ft}^{-1}$ ,  $\omega = 12 \text{ rad/sec}$  with the variation of the reciprocal of the latus rectum  $c$ .

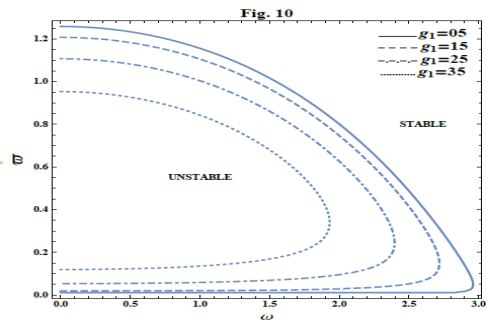


**Fig. 10.** Depicts the transition curve that is given in Equation (71) for a system having the particulars:  $g_0 = 32 \text{ ft/sec}^2$ ,  $c = 0.1 \text{ ft}^{-1}$  with the coefficient of the excitation force  $g_1$ .

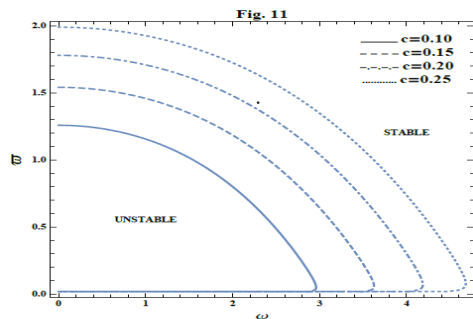


**Fig. 11.** Depicts the transition curve that is given in Equation (71) for a system having the particulars:  $g_0 = 32 \text{ ft/sec}^2$ ,  $g_1 = 5 \text{ ft/sec}^2$  with the reciprocal of the latus rectum  $c$ .

## 8. Concluding remarks

The present study investigates the motion of a sliding bead on a smooth wire which is bent in the shape of a vertical parabola of the form  $z = cr^2$ . The parabola rotates around its vertical axis with uniform angular velocity  $\omega$ . By making use of the Euler-Lagrange approach, the governing equation of motion is achieved. The coupling of the HPM and  $L_T$  is utilized to obtain an approximate solution. Unfortunately, this approach does not enable us to avoid the secular terms. It is evident that this cancellation resulted in the trivial solution, which is valid but not desired. Therefore, the obtained approximate solution is unstable for a long time. On the other hand, an approximate periodic solution is obtained via the expanded frequency analysis together with the coupling of the HPM and  $L_T$ . In fact, the latter approach can be characterized as powerful, promising and straightforward. It may be applied to highly nonlinear problems. Through this approach, the stability criterion is obtained. The dispersion equation is also achieved. It represents a quadratic algebraic equation in the artificial frequency  $\Omega^2$ . By means of HPM, an approximate solution is obtained. Furthermore, the analyses reveal an external excitation which is based on an oscillatory gravitational force. For this purpose, the stability analysis of the problem is investigated by the use of multiple time-scales with HPM. The non-resonance case reveals a Landau equation, which shows that the system is always stable. Because this mode does not enable us to judge the stability/instability of the system, we proceed to investigate the resonance case. In order to make the stability analysis more profound, the linearization techniques are used in order to check the stability of the linearized equation and then compare the finding with those from the multiple time-scales method results. The outcomes of the present work may be summarized as follows:

- The classical approximate solution, involving the secular terms is given by Equation (18).
- The periodic approximate solution, based on the expanded frequency is given by Equation (32).
- The characteristic equation of the expanded frequency is defined in Equation (33).
- The stability criterion in the case of expanded frequency is given by Equation (36).
- The periodic approximate solution, based on the multiple time scales in the non-resonance case, is given by Equation (56).

- Several figures display the effects of the various physical parameters in the approximate perturbed solutions as well as the stability criteria.
- The numerical calculations, in the previous two cases, show that the angular frequency and the initial linear velocity have a destabilizing influence.
- In contrast, the parameter  $c$ , which represents the reciprocal of the latus rectum, has a stabilizing effect.
- The multiple time scale analysis resulted in a transition curve as given by Equation (67).
- In contrast with the non-resonant case, the linearization techniques of stability, in the autonomous case, resulted in some stability criteria.
- In the non-autonomous case, several transition curves were obtained.
- The examination of the external excitation shows that the parameter  $c$  has a stabilizing influence. In contrast, the coefficient of the excitation term has a destabilizing influence.

## ACKNOWLEDGEMENTS

Many thanks to Prof. H. Yehia (Mansoura University, Egypt) for his interest and useful feedback.

## References

- Ali, F., Sheikh, N.A. Khan, I. & Saqib, M. (2017). Solutions with Wright function for time fractional free convection flow of Casson fluid, *Arabian Journal of Science and Engineering*, **42**(6): 2565-2572.
- Ayati, Z. & Biazar, J. (2015). On the convergence of homotopy perturbation method. *Journal of the Egyptian Mathematical Society*, **23**(2): 424-428.
- Bayat, M., Pakar, I. & Bayat, M. (2015). Nonlinear vibration of mechanical systems by means of homotopy perturbation method. *Kuwait Journal of Science*, **42**(3): 64-85.
- Coddington, E.A. & Levinson, N. (1977). *Theory of Ordinary Differential Equations*. McGraw-Hill, New Delhi.
- Dao, N.V., Dinh, N.V.T. & Chi, K. (2007). Van der Pol oscillator under parametric and forced excitation. *Ukrainian Mathematical Journal*, **59**(2): 215-228.
- Demiray, S.T. & Bulut H. (2017). New exact solution for generalized Gardner equation. *Kuwait Journal of Science*, **44**(1): 1-8.
- El-Dib, Y.O. (2017). Multiple scales homotopy perturbation method for nonlinear oscillators. *Nonlinear Science Letters A*, **8**(4): 352-364.
- El-Dib, Y.O. & Moatimid, G.M. (2018). On the coupling of the homotopy perturbation and Frobenius method for exact solutions of singular nonlinear differential equations. *Nonlinear Science Letters A*, **9**(3): 220-230.
- El-Dib, Y.O., Moatimid, G.M., (2019). Stability configuration of a rocking rigid rod over a circular surface using the homotopy perturbation method and Laplace transform. *Arabian Journal of Science and Engineering*, **44**(7): 6581-6591.
- Filobello-Niño, U., Vázquez-Leal, H., Khan, Y., Sandoval-Hernandez, M., Perez-Sesma, A., Sarmiento-Reyes, A., Benhammouda, B., Jimenez-Fernandez, V.M., Huerta-Chua, J., Hernandez-Machuca, S.F., Mendez-Perez, J.M., Morales-Mendoza, L.J. & Gonzalez-Lee, M. (2017). Extension of Laplace transform-homotopy perturbation method to solve nonlinear differential equations with variable coefficients defined with Robin boundary conditions. *Neural Computing & Applications*, **28**(3): 585-595.
- He, J.H. (1999). Homotopy perturbation method. *Computer Methods in Applied Mechanics Engineering*, **178**(3-4): 257-262.
- He, J.H. (2000). A coupling method of homotopy technique and perturbation technique for nonlinear problems. *International Journal of Nonlinear Mechanics*, **35**(1): 37-43.
- He, J.H. (2000). A new perturbation technique which is also valid for large parameter. *Journal of Sound Vibration*, **299**(5): 1257-1263.
- Ibrahim, R.A. (1985). *Parametric random vibration*. John Wiley & Sons, New York.
- Kaliji, H.D., Ghadimi, M. & Eftari, M. (2013). Investigating the dynamic behavior of two mechanical structures via analytical methods. *Arabian Journal of Science and Engineering*, **38**: 2821-2829.
- Maiybaev, A.A. (2002). On stability domains of neoconservative systems under small parametric excitation. *Acta Mechanica* **154**: 11-30.
- Moatimid, G.M., Obied Allah, M.H. (2010).

Electrohydrodynamic linear stability of finitely conducting flows through porous fluids with mass and heat transfer. *Applied Mathematics Modelling*, **34**(10): 3118-3129.

Nayfeh, A.H. (1973). *Perturbation Methods*. Wiley, New York.

Nayfeh, A.H. & Mook, D.T. (1979). *Nonlinear Oscillations*. Wiley-Interscience, New York.

Neves, A. (2009). Floquet's theorem and stability of periodic solitary waves. *Journal of Differential Equations*, **21**(3): 555-565.

Schiff, J.L. (1999). *The Laplace Transform (Theory and Applications)*, Springer-Verlag Inc, New York.

Thornton, S.T. & Marion, J.B. (2004). *Classical Dynamics of Particles and Systems*, 5<sup>th</sup> Edition. Brooks/Cole-Thomson Learning, USA.

Wu, B.S., Lim, C.W. & He, L.H., (2003). A new method for approximate analytical solutions to nonlinear oscillations of non-natural system. *Nonlinear Dynamics*, **32**(1): 1-13.

**Submitted** : 30/09/2018

**Revised** : 17/04/2019

**Accepted** : 18/04/2019